## PUBLICATION N° 4

## Molecular and Cellular Biology (Mol. Cell Biol)


**Auteurs: Capo-Chichi CD,** Cai KQ, Testa JR, Godwin AK, Xu XX.

**Titre**: Loss of GATA6 Leads to Nuclear Deformation and Aneuploidy in Ovarian Cancer.
Mol Cell Biol. 2009 Sep; 29(17): 4766–4777. doi: 10.1128/MCB.00087-09
**Print ISSN**: 0270-7306, **Online ISSN**: 1098-5549

**Impact Factor (Factor impact) :** 3,735

**Indexation**

Agricola, BIOSIS Previews, Biotechnology Citation Index, CAB Abstracts, Cambridge Scientific Abstracts, Chemical Abstracts Service, Current Contents- Life Sciences, EMBASE, MEDLINE

**Lien d'indexation: https://mcb.asm.org/content/about-mcb**

**Lien de l'article : https://mcb.asm.org/content/29/17/4766**

**Web: https://www.asm.org/**

https://pubmed.ncbi.nlm.nih.gov/19581290/

MOLECULAR AND CELLULAR BIOLOGY, Sept. 2009, p. 4766–4777 Vol. 29, No. 17
0270-7306/09/$08.00+0 doi:10.1128/MCB.00087-09


# Loss of GATA6 Leads to Nuclear Deformation and Aneuploidy in Ovarian Cancer▽†

Callinice D. Capo-chichi,[1,2] Kathy Q. Cai,[2] Joseph R. Testa,[2] Andrew K. Godwin,[2] and Xiang-Xi Xu[1,2]*

*Sylvester Comprehensive Cancer Center, Department of Medicine, and Department of Obstetrics and Gynecology, University of Miami School of Medicine, Miami, Florida 33136,[1] and Ovarian Cancer, Human Genetics, and Tumor Cell Biology Programs, Fox Chase Cancer Center, Philadelphia, Pennsylvania 19111[2]*

Received 19 January 2009/Returned for modification 23 February 2009/Accepted 25 June 2009

**A prominent hallmark of most human cancer is aneuploidy, which is a result of the chromosomal instability of cancer cells and is thought to contribute to the initiation and progression of most carcinomas. The developmentally regulated GATA6 transcription factor is commonly lost in ovarian cancer, and the loss of its expression is closely associated with neoplastic transformation of the ovarian surface epithelium. In the present study, we found that reduction of GATA6 expression with small interfering RNA (siRNA) in human ovarian surface epithelial cells resulted in deformation of the nuclear envelope, failure of cytokinesis, and formation of polyploid and aneuploid cells. We further discovered that loss of the nuclear envelope protein emerin may mediate the consequences of GATA6 suppression. The nuclear phenotypes were reproduced by direct suppression of emerin with siRNA. Thus, we conclude that diminished expression of GATA6 leads to a compromised nuclear envelope that is causal for polyploidy and aneuploidy in ovarian tumorigenesis. The loss of emerin may be the basis of nuclear morphological deformation and subsequently the cause of aneuploidy in ovarian cancer cells.**

Although derived from host cells, cancer cells have distinctive characteristics, and many hallmarks of cancer cells have been well recognized and understood (19, 43). The basis for the malignant transformation has been well accepted to be genetic changes (19), and progressive accumulation of mutations in oncogenes and tumor suppressor genes has been recognized to underlie tumor development (14, 24, 50). The majority of cancer cells are aneuploid and possess a different and unbalanced number of chromosomes than normal cells as a result of gain or loss of individual chromosomes during malignant transformation (28, 42, 49). The correlation between aneuploidy and malignancy was recognized nearly 100 year ago (4), yet the causes and significance of aneuploidy in cancer remain unsettled (21, 51). Several mechanisms for the origination of aneuploidy have been noted (21). Genes that cause mitotic failure account for the majority of cases. Tetraploid cells are believed often to form following mitotic failure, and aneuploid cells are produced in subsequent mitotic events (16, 32, 48). In vitro, cultured cells can be transformed to tumorigenic cells by mutations and deletion of individual genes (oncogenes and tumor suppressor genes), even without chromosomal instability (55). Nevertheless, the common occurrence of aneuploidy in human cancer cells suggests that it has an important role in the development of human cancer (34, 41). Indeed, it was reported that drug-induced cytokinesis failure generates tetraploids that promote tumorigenesis in p53-null mammary epithelial cells (15).

One unique view is that chromosome instability and aneuploidy may provide an unbalanced global expression profile of increases and decreases in gene dosages that create cancer cell properties (13). A general interpretation is that chromosome instability and aneuploidy may promote the accelerated loss and gain of specific tumor suppressor genes and oncogenes, respectively, leading to malignant transformation (34, 28, 40). In either case, aneuploidy likely plays important roles in cancer initiation and progression.

Because of the increased number of chromosomes, the nuclei of cancer cells are often enlarged and also often exhibit a deformed morphology, in contrast to the oval shape of normal cells (56). As a result, nuclear morphology is a useful diagnostic marker for tumor malignancy (12). Yet, although the importance of the altered nuclear morphology in neoplasia has been speculated about (1, 38, 56), our molecular understanding of the causes and significance of nuclear morphological deformation of cancer cells is very limited.

In this study, we discovered a surprising link between the causes of nuclear deformation and aneuploidy of cancer cells, following our investigation of the consequence of the loss of GATA6 in ovarian surface epithelial cells. GATA6 is a developmentally regulated transcription factor that functions in early embryonic stem cell differentiation (5, 9), and genetic knockout in mice leads to early embryonic lethality (5, 25, 36). GATA6 is also a key factor in determining cell lineages in subsequent embryonic development and organogenesis of many tissue types (35). GATA6 expression was found to be lost in the majority of ovarian cancer cells, and it was proposed that the loss of GATA6 accounts for the epithelial dedifferentiation of ovarian cancer cells (8). Alteration of chromatin conforma-

* Corresponding author. Mailing address: University of Miami School of Medicine, Rm. 417, Papanicolaou Building, 1550 NW 10th Ave. (M710), Miami, FL 33136. Phone: (305) 243-1750. Fax: (305) 243-5555. E-mail: xxu2@med.miami.edu.

† Supplemental material for this article may be found at http://mcb.asm.org/.

▽ Published ahead of print on 6 July 2009.

tion is one mechanism for the loss of GATA6 expression in ovarian cancer (10).

Our experiments to determine the phenotype of GATA6 loss in ovarian epithelial cells led to the findings that loss of GATA6 causes nuclear deformation and the development of aneuploidy and that loss of nuclear envelope protein may mediate the process.

## MATERIALS AND METHODS

**Cell cultures.** Human ovarian surface epithelium (HOSE) cells were established from ovaries obtained from prophylactic oophorectomies at local hospitals (8, 10). HOSE cells were transfected with simian virus 40 T antigen to prepare human ''immortalized'' ovarian (HIO) cells. These HIO cells have a longer life span in culture and can be cultured for 20 to 50 passages before undergoing senescence, compared to HOSE cells, which can only be maintained for 7 to 10 passages.

Cancer cells were typically cultured in T75 flasks in RPMI 1640 medium supplemented with 10% fetal bovine serum and 100 U/ml penicillin-streptomycin at 37°C in a humidified atmosphere of 5% $CO_2$.

Caspase-6 inhibitor (A6339, *N*-acetyl-Val-Glu-Ile-Asp-al) and proteasome inhibitor (L7035, clasto-lactacystin b-lactone) were purchased from Sigma, Inc. The inhibitors were used to treat cells according to the general protocol provided by the commercial source.

**Antibodies, immunofluorescence microscopy, and immunostaining.** A primary antibody against GATA6 was produced against the peptide sequence of human GATA6 (amino acids 10 to 25 [accession no. U66075.1] or 156 to 171 [accession no. NM_005257.3]), GATA6 SQGPA AYDGA PGGFV H, in rabbits. This peptide was also found to be identical in mice, and the antibodies also show strong and specific reactivity to the mouse protein (5). The antiserum was characterized and used at a 1/5,000 dilution for immunohistochemical staining, a 1/1,000 dilution for immunoblotting, and a 1/500 dilution for immunofluorescence microscopy. Additional antibodies were purchased from commercial sources: Mouse antiemerin, goat anti-lamin B, goat anti-Baf, and mouse anti-lamin A/C antibodies were purchased from Santa Cruz Biotechnology, Inc. (Santa Cruz, CA); mouse anti-Dab2 antibody was purchased from BD Biosciences. The general procedures and conditions for immunostaining were detailed previously (8).

For immunofluorescence microscopy, cells were fixed with 4% paraformaldehyde for 15 min, permeabilized with 0.5% Triton X-100 for 5 min, blocked with 3% bovine serum albumin in phosphate-buffered saline (PBS) containing 0.1% Tween 20 for 30 min, and incubated for 1 h at 37°C with primary antibodies. The nuclei and chromosomes were stained blue with Hoechst 33342 solution (1 μM) or 4′,6-diamidino-2-phenylindole (DAPI). Fluorescent Alexa Fluor 488- and 596-conjugated secondary antibodies (used at a 1/500 dilution) and Hoechst 33342 nuclear counterstaining dye (used at 1 μM) were purchased from Molecular Probes (Eugene, OR). Cells were washed three times and covered with antifade reagent containing 0.1 M *n*-propyl gallate (pH 7.4) and 90% glycerol in PBS. Immunofluorescence staining was viewed with a 20×, 60×, or 100× (oil) objective lens on a Nikon Eclipse TE 300 microscope linked to a Roper Scientific photometrics camera with a 12-bit range. Image acquisition was done with Meta Imaging Series (MetaVue) software. Images were merged by using MetaVue software.

**Measurement of gene expression by RT-PCR.** Real-time PCR was used to quantify mRNA levels following reverse transcription (RT). The protocol used was described in detail in a previous report (10).

**Small interfering RNA (siRNA) and short hairpin RNA (shRNA).** For transient transfection, a custom siRNA directed against the 21 nucleotides of the human GATA6 sequence, 5′ AACTG CGGCT CCATC CAGAC G 3′, was purchased form Ambion (Austin, TX). This sequence was the most efficient in suppressing GATA6 among many tested previously (8). A mixture of several oligonucleotides of siRNA specific to ermine, lamin A/C, or lamin B was purchased from Santa Cruz, Inc. The siRNA oligonucleotides were transfected with Lipofectamine 2000 (Invitrogen, CA) in serum-reduced Opti-MEM medium according to the manufacturer's recommendation. Control cells were transfected with scrambled siRNA.

For stable transfection, a GATA6 shRNA expression vector in IMG800 (Imgenex, Inc.) was used and stable clones were obtained after selection of cells in medium containing 1 mg/ml G418 for 21 days. Details were published previously (8).

**Time-lapse video microscopy.** Time-lapse image acquisition of cells expressing histone H2B-green fluorescent protein (GFP) (23) was done on the green fluorescence channel by bright-field microscopy every 5 min for 24 h with a 40× objective lens. Stacked images were assembled with MetaVue software to produce movies.

**Flow cytometric analysis.** Cells were washed once with PBS, trypsinized with 0.04% trypsin solution, and then fixed by resuspending the pellet in ice-cold ethanol (70%, vol/vol) in PBS with gentle agitation, and the cells were kept at −20°C until ready to use. Before flow cytometric analysis, the cells were suspended in propidium iodide and RNase A solution (20 and 200 mg/ml, respectively) and incubated at 37°C for 30 min. Cell sorting and flow cytometric analyses were performed on a FACS Vantage SE machine with Diva (digital vantage) software (Becton Dickinson, San Jose, CA). Live-cell sorting was done in fresh medium containing 0.5 μmol of Vybrant violet dye (Molecular Probes, Inc.).

**Cytogenetic analysis.** Chromosome number counting was performed by the Fox Chase Cancer Center Research Cytogenetics Core Facility. The cells were exposed to colcemid for 3 to 12 h and harvested with 0.075 M KCl and methanol-acetic acid (3:1). Fifty metaphases were analyzed in the control or GATA6-suppressed samples, and the experiments were performed in duplicate with six different HOSE cell preparations.

## RESULTS

**Suppression of GATA6 leads to nuclear morphological deformation and aneuploidy in ovarian surface epithelial cells.** GATA6 was previously found to be lost in the majority of ovarian cancers (8). To determine the consequence of GATA6 elimination in cell culture, we suppressed GATA6 expression by siRNA or shRNA in primary HOSE and nontumorigenic HIO cells (8). The GATA6 siRNA treatment caused nearly complete suppression of GATA6 protein over the 2- to 5-day period, as reported previously (8). Within 2 to 3 days after targeting GATA6 with siRNA, we observed a dramatic occurrence of cells with large and irregularly shaped nuclei (Fig. 1A). In several experiments with multiple HOSE cell preparations, GATA6 downregulation consistently resulted in nearly 65% of the cells having a large and atypical nuclear morphology. Conversely, cells transfected with control siRNA exhibited smooth, round or oval nuclei with a background of cells having atypical nuclei of less than 4%. The effect of GATA6 downregulation on the cell size and morphology of the whole population was also revealed by flow cytometric analysis (Fig. 1B). Presumably, the size and shape of cells reflect the changes in size and shape of the nucleus. GATA6 downregulation caused a shift of the cell population toward larger and irregular shapes, as indicated by forward (FSC-H) and sideward (SSC-H) light scattering, respectively. Additionally, the GATA6-suppressed cells were aneuploid or polyploid, as determined by cell cycle flow cytometry (Fig. 1C). In this experiment, the 4n cell-containing P3 fractions were collected by flow cytometry with Vybrant violet dye as a DNA content indicator in both vector control (16% in P3) and shRNA GATA6-suppressed (36% in P3) cells. After culturing for an additional 7 weeks, the entire cell population was again analyzed by flow cytometry. In control shRNA-treated cells, the majority of the cells redistributed back to 2n stages (22% in P3), indicating that the previously collected P3 fraction of the 4n cells was in the $G_2$/M phase (Fig. 1C). In contrast, the GATA6-suppressed cells in the P3 fraction largely remained in 4n and also 8n stages (86% in P3) following prolonged culturing (7 weeks), suggesting that the collected 4n cells were mostly tetraploid (Fig. 1C). Thus, most of the GATA6-suppressed cells with larger than 2n DNA content were not pro-

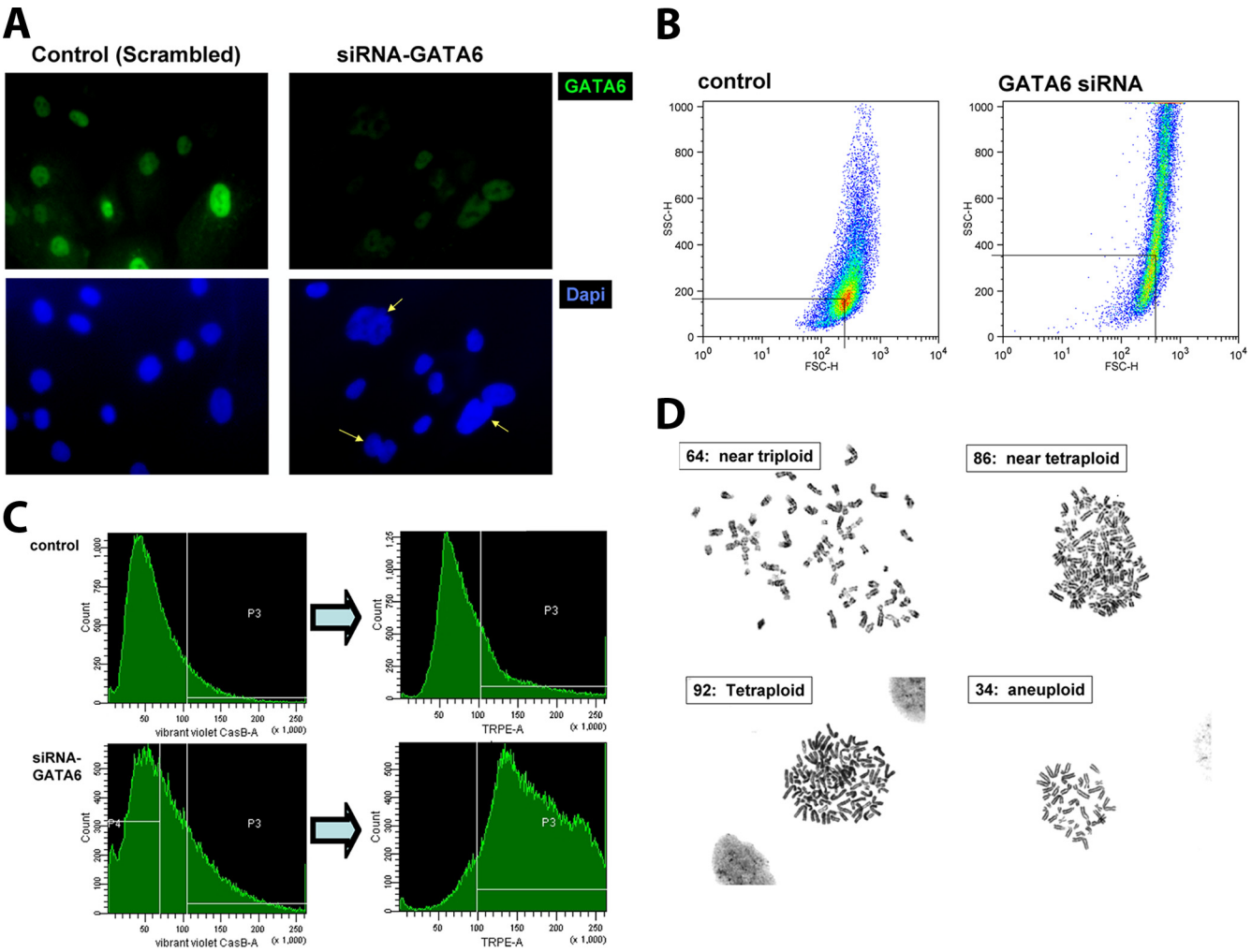


FIG. 1. Suppression of GATA6 in HOSE cells leads to nuclear defects and polyploidy. GATA6 expression was suppressed by either an shRNA expression vector or siRNA oligonucleotides in HOSE and HIO cells. (A) Nuclear morphology was examined following DAPI staining 3 days after the addition of siRNA oligonucleotides targeting GATA6 to HOSE cells. Large and irregular nuclei (arrows) were observed in GATA6-suppressed cells but not in control cells. (B) Alteration of cell size and morphology was confirmed by flow cytometry of forward and sideward light scattering (FSC-H and SSC-H, respectively). The entire population of GATA6-suppressed HOSE cells exhibited a shift to bigger and irregularly shaped cells. (C) Flow cytometric analysis. HIO-114 cells were transfected with a control or shRNA-GATA6 vector and cultured in the presence of G418. The G418-resistant cells selected were sorted by flow cytometry in the presence of Vybrant violet dye as an indicator of the DNA content of live cells. The 4n cell-containing P3 fraction was collected and cultured for 7 weeks before analysis by flow cytometry. (D) Metaphase spreads of GATA6-suppressed HOSE cells. HOSE cells were transfected with a control or shRNA-GATA6 vector and subjected to cytogenetic analysis on days 3 and 7. To obtain metaphases, the cell were exposed to colcemid for 3 to 12 h, treated with 0.075 M KCl, and fixed in methanol-acetic acid (3:1). Fifty consecutive chromosome spreads of each sample were selected for chromosome counting. Four representative metaphase spreads are shown. Similar results were observed in six independent HOSE cell preparations.

liferating S-phase or M-phase cells but rather were aneuploid or polyploid cells.

The formation of polyploid and aneuploid cells was also demonstrated by cytogenetic analysis. At day 3 following transfection with the GATA6 siRNA vector (with a 20% transfection efficiency, as indicated by cotransfected GFP expression vectors), a significant percentage of metaphase chromosome spreads were found to be aneuploid and polyploid. In representative metaphase spreads of HOSE cells from a consecutive counting, 7 (14%) of 50 spreads were nearly tetraploid (84 to 92 chromosomes). By day 7, the presence of aneuploid cells increased further; 2 tetraploid spreads and 5 aneuploid spreads with chromosome counts of 26 to 45 were found among the 50 spreads counted, representing 16% aneuploid or tetraploid spreads. Representative metaphase spreads are shown in Fig. 1D. In 50 metaphases from the cells transfected with the control siRNA vector, only one tetraploid spread was counted at day 3 and one nearly diploid spread (45 chromosomes) was found at day 7, and all other metaphase spreads had normal diploid counts. Thus, GATA6 suppression causes a dramatic increase in the formation of polyploid and aneuploid cells. The extent of aneuploidy in metaphase spreads observed likely was an underestimation due to limited transfection efficiency and the fact that the cytogenetic analysis is limited to dividing cells. Indeed, we found significantly fewer metaphase chromosome spreads in GATA6-suppressed than control cultures.

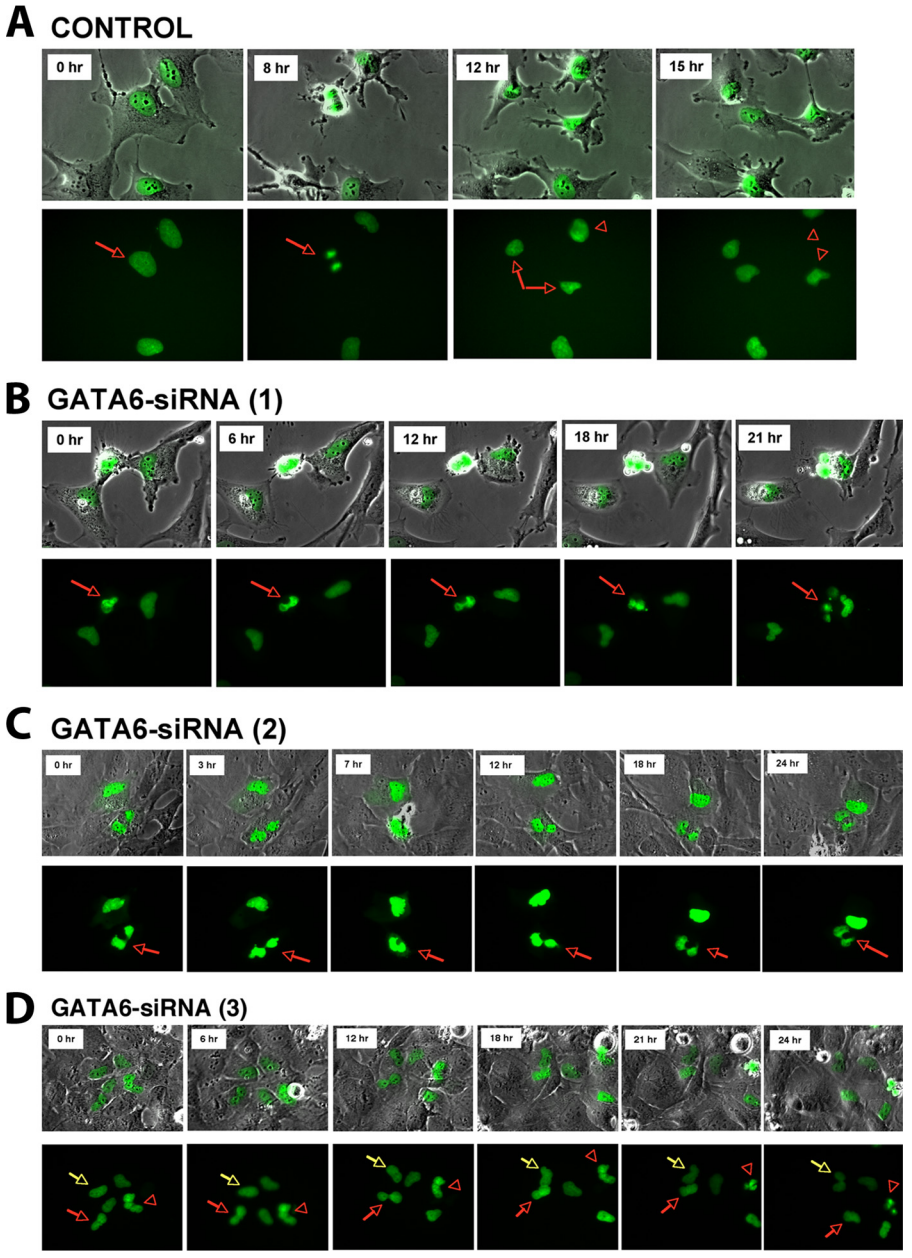


FIG. 2. Suppression of GATA6 leads to mitotic failure in HIO and HOSE cells. An shRNA-GATA6 suppression vector and a histone H2B-GFP expression construct were cotransfected into HOSE or HIO-80 cells. Time-lapse video microscopy was used to monitor the mitotic phenotype of GFP-expressing cells for 24 h following transfection. GFP and the corresponding phase-contrast images of the time course obtained from the time-lapse video are shown. (A) Cells cotransfected with a control (scrambled) shRNA vector showed completion of cytokinesis and mitosis. Two examples of mitosis are indicated by arrows and arrowheads. (B) Example (indicated by an arrow) of GATA6-suppressed HIO-80 cells showing that the condensed chromatin failed to separate and ultimately the furrow regressed and the nuclei fractured to form micronuclei. (C) Example (indicated by an arrow) of GATA6-suppressed cells showing persistence of repeated chromosome segregation and furrow regression. (D) Serial images of a video of GATA6-suppressed cells showing that the dividing nucleus either regressed to form a 4n nucleus (red arrow), broke down to form micronuclei (red arrowhead), or formed two nuclei linked by a chromatin bridge (yellow arrow).

In experiments completed over an 18-month period, the effects of GATA6 suppression on nuclear morphology were replicated in 10 different HOSE cell preparations. Additionally, similar and/or more dramatic effects of GATA6 downregulation were observed in HIO-80, HIO-105, and HIO-114 cells, which are ovarian surface epithelial cells transfected with simian virus 40 T antigen to prolong the life span of the cells in culture (8). The HIO cells were suitable to be used for transfection with shRNA vector and selection of stable clones of GATA6 suppression. Thus, the development of aneuploidy/polyploidy and nuclear morphology abnormalities in primary HOSE and HIO cells following GATA6 suppression is reproducible and robust.

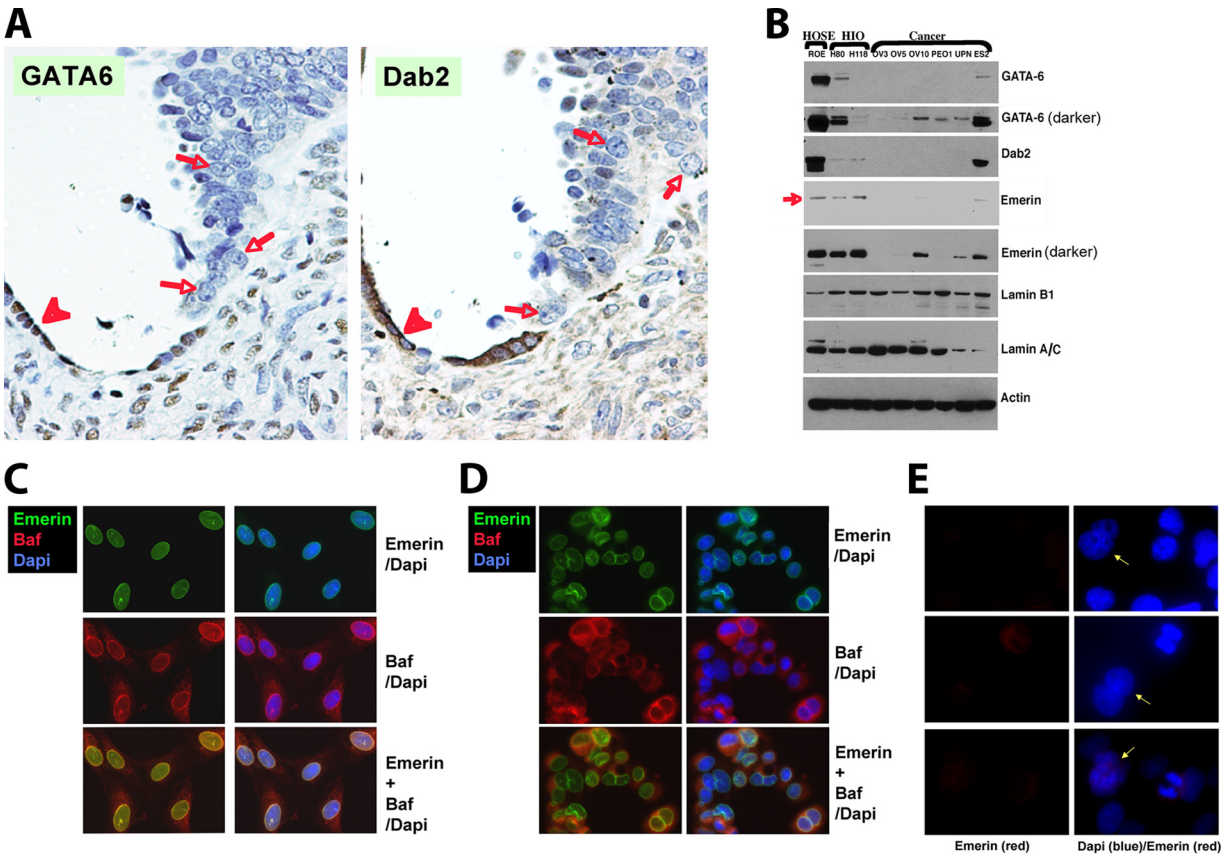


FIG. 3. Nuclear defect and loss of GATA6 in ovarian cancer cells. (A) Loss of GATA6 is associated with enlargement and misshaping of the nucleus in malignant ovarian cancer cells. Adjacent sections of ovarian carcinomas were immunostained with GATA6 and its transcription target, Dab2. Shown is an example of the coexpression of GATA6 and Dab2 in morphologically normal ovarian surface epithelial cells (arrowhead) and loss of expression of both GATA6 and Dab2 in concurrence with altered nuclear morphology in malignant cells (arrows). More than 20 such cases of a contiguous epithelium linking morphologically normal and neoplastic cells were observed to show a correlation between the loss of GATA6 and nuclear morphological changes. (B) Western blot analysis of GATA6, Dab2, and nuclear envelope proteins, including emerin, lamin A/C, and lamin B, in a panel of HOSE, HIO, and cancer cells. A darker exposure of the Western blot for GATA6 and emerin showed the presence of a small amount of the proteins in several cancer lines. (C) Immunofluorescence analysis of HIO-80 cells. Cells were stained for emerin (green) and Baf (red). DAPI (blue) staining was used to visualize the nuclei. (D) Immunofluorescence analysis of OV10 ovarian cancer cells for emerin (green), Baf (red), and DAPI (blue) staining. (E) Immunofluorescence analysis of OV5 ovarian cancer cells illustrating emerin (red) and nuclear DAPI (blue) staining. Three examples are shown, and atypical nuclei are indicated (arrows).

**Suppression of GATA6 in ovarian surface epithelial cells leads to mitotic failure that is the cause of the formation of tetraploidy and aneuploidy.** Next, we cotransfected the shRNA-GATA6 suppression vector with a histone H2B-GFP expression construct (23) to label chromosomal DNA and examined the cells over a 24-h period by time-lapse video microscopy to observe the causes of abnormal nuclear morphology in HIO cells. In more than 20 videos made of four independent transfections, we observed that in every instance when a cell was cotransfected with shRNA-GATA6 and histone H2B-GFP, the GFP-expressing cell failed to divide in mitosis and acquired an enlarged and aberrant nuclear morphology. GFP-expressing cells cotransfected with the control siRNA vector, however, completed cytokinesis and mitosis (Fig. 2A). Three typical phenotypes were observed in GATA6 siRNA-transfected cells (Fig. 2B, C, and D; for time-lapse videos, see the supplemental material). As shown in Fig. 2B, a transfected cell (arrow) progressed to metaphase/anaphase morphology by 6 h in the video. However, the dividing DNA failed to resolve the chromatin bridge, which persisted for 12 more h. At 18 h, the furrow regressed, and by 21 h, the nucleus fractured to form micronuclei. In a second example (Fig. 2C), a dividing nucleus (arrow) regressed by 7 h, attempted to segregate again at 12 h, and persisted until 24 h. In a third example (Fig. 2D), several cells showed the process of failed cytokinesis. A dividing nucleus regressed to form a 4n nucleus (red arrow), another dividing nucleus condensed but then broke down to form micronuclei (red arrowhead), or the last dividing cell formed two nuclei linked by a chromatin bridge (yellow arrow). In all, time-lapse analysis indicated that abnormally large and irregular nuclei formed due to failure of cytokinesis or mitosis following GATA6 suppression. Thus, we conclude that mitotic defects and failure of cytokinesis are the causes of the formation of tetraploid cells and deformed nuclei following suppression of GATA6.

**Loss of GATA6 and emerin and nuclear deformation in ovarian cancer.** We further examined the relationship between GATA6 expression and nuclear morphology in ovarian cancer

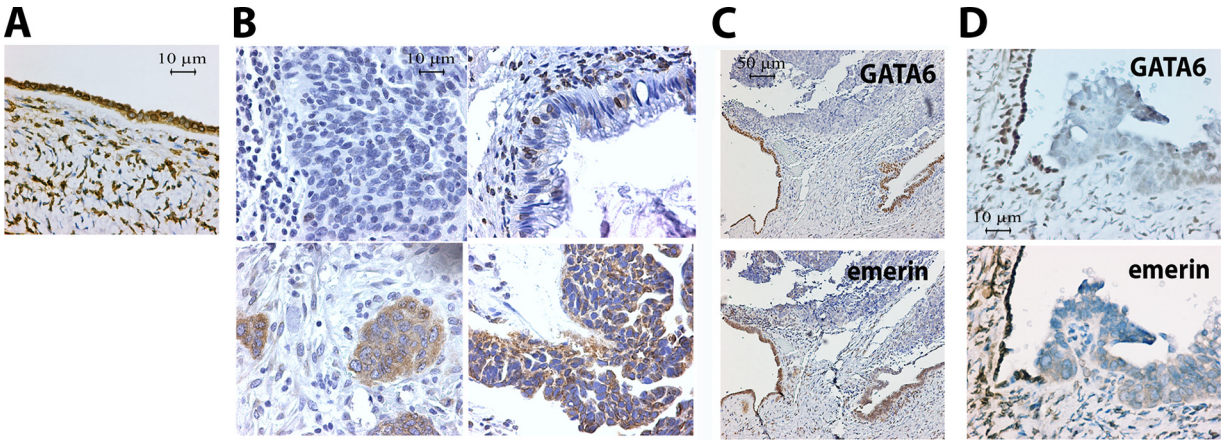


FIG. 4. Loss of emerin expression in ovarian cancer cells. (A) Immunostaining of emerin in human ovary tissue. Representative emerin staining of normal human ovary tissue is shown. Emerin staining is intensively positive around the nuclear envelope of ovarian surface epithelial cells. (B) Immunostaining of emerin in four representative ovarian adenocarcinomas. Staining is (clockwise) completely absent, heterogeneous, abnormal (patchy), or cytoplasmic. Shown is an example of an ovarian carcinoma containing noncancerous ovarian surface epithelial cells and transformed cells. The nonneoplastic epithelial cells are GATA6 and emerin positive, and cancer cells are negative for GATA6, correlating with the absence of emerin staining. (C) Example of an ovarian carcinoma containing noncancerous ovarian surface epithelial cells and transformed cells. The nonneoplastic epithelial cells are GATA6 and emerin positive, and cancer cells are negative for GATA6, correlating with the absence of emerin staining. (D) Example of an ovarian cancer lesion containing contiguously linked noncancer ovarian surface epithelial cells and malignant cells. The loss of GATA6 expression correlates well with loss of emerin and morphological transformation.

tissues. In all of 16 cases of ovarian carcinomas in which monolayers of ovarian surface epithelial cells linked contiguously with malignant cells were present (53), we found that loss of GATA6 expression is associated with loss of Dab2 protein and the morphological transformation of monolayer ovarian surface epithelial cells (arrowhead) to carcinoma cells (arrow) (an example is shown in Fig. 3A). Additionally, loss of GATA6 also correlates with enlarged and misshapen nuclei in malignant ovarian cancer cells (Fig. 3A, arrows), consistent with the above observation in culture cells.

Because of the unique nuclear deformation of the GATA6-suppressed HOSE cells and GATA6-negative cancer cells, we examined the nuclear envelope integrity of ovarian cancer cells. Several nuclear envelope proteins are known to be critical for the maintenance of nuclear shape (26, 27, 44). We reasoned that the loss of a nuclear envelope protein following loss of GATA6 might be the cause of the nuclear phenotypes observed and examined the expression of several nuclear envelope proteins in ovarian epithelial and cancer cells (Fig. 3B). In a panel of ovarian surface epithelial and cancer cells examined by Western blotting, GATA6 was often lost, correlating with loss of expression of its transcription target, Dab2 (8, 10) (Fig. 3B). Among several nuclear envelope proteins examined, emerin, which was initially identified as the product of an X-linked gene responsible for Emery-Dreifuss muscular dystrophy (2, 37), was absent or greatly reduced in many cancer cell lines, although a smaller amount of emerin was detectable in a darker exposure of the Western blot in several cancer cell lines (Fig. 3B). A darker exposure of the Western blot for GATA6 also showed the presence of some GATA6 protein in the corresponding cell lines (Fig. 3B). In HIO-118 cells (Fig. 3C) and emerin-positive NIHOVCAR10 (OV10) ovarian cancer cells (Fig. 3D), emerin immunofluorescence staining showed a nuclear envelope localization and a smooth, oval-shaped nucleus. Moreover, emerin staining overlapped with that of Baf (barrier to autointegration factor), an emerin-binding nuclear envelope protein (47). The nuclei of OV10 cells are abnormal in a unique manner in that two enveloped nuclei are often closely associated (Fig. 4D). In emerin-negative NIHOVCAR5 (OV5) ovarian cancer cells, the absence of emerin was associated with a high percentage (approximately 20%) of cells possessing large and irregularly shaped nuclei (Fig. 3E). Loss of emerin is known to cause nuclear morphological deformation (27, 44), suggesting that absence of emerin may be the cause of nuclear deformation in ovarian cancer cells.

It was noticed that in HIO-118 cells, GATA6 expression is very low, although emerin expression is present, indicating that an exception to the correlation between GATA6 and emerin expression exists (Fig. 3B).

In human ovarian tissues, ovarian surface epithelial cells are intensely stained with emerin around the nuclei (Fig. 4A). We found that emerin immunostaining was completely absent in 32 (38%) of the 84 ovarian adenocarcinomas examined in tissue microarrays (Fig. 4B). Additionally, most of the emerin-positive tumors showed abnormal emerin expression patterns, such as heterogeneous staining of cells or staining that was not localized to the nuclear envelope but instead distributed in the cytoplasm (Fig. 4B). Thus, the loss or abnormal distribution of emerin occurs in a significant percentage of human ovarian cancers.

Furthermore, in another 12 cases of ovarian cancer in which contiguous epithelia linking morphologically normal monolayer ovarian surface epithelial cells and multilayer cancer cells are present, a close correlation between the loss of GATA6 and the loss of emerin was observed, as shown in an example in Fig. 4C. In regions containing contiguous epithelia linking benign and neoplastic cells, the loss of GATA6 correlates well with the loss of emerin and epithelial and nuclear morphological transformation (Fig. 4D).

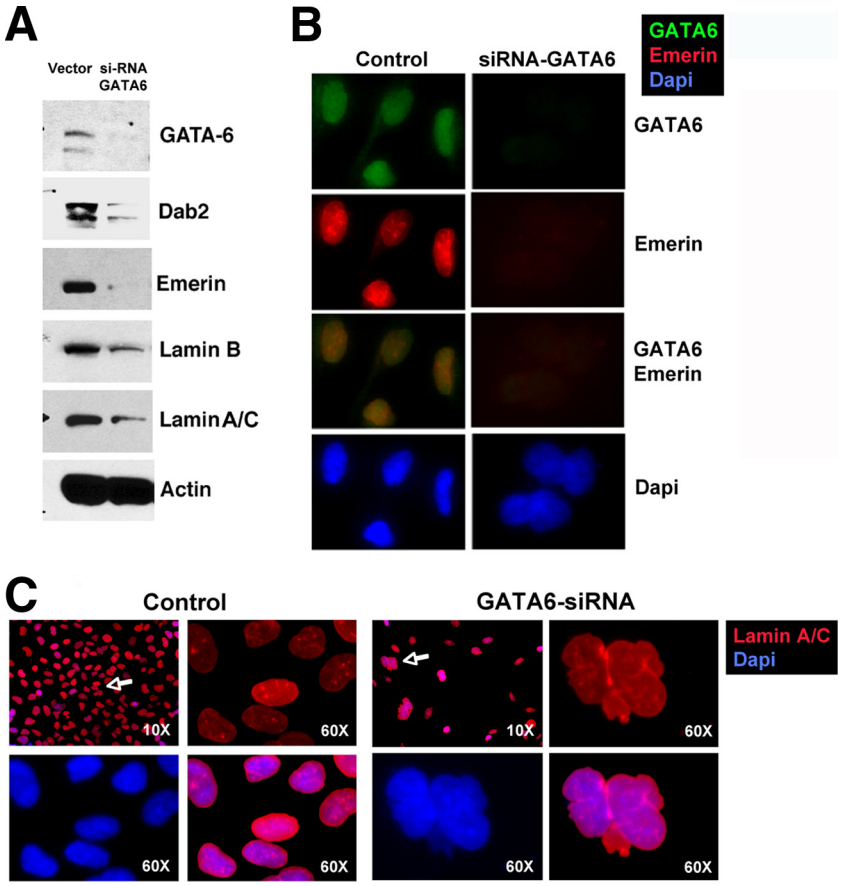


FIG. 5. Loss of emerin following GATA6 suppression by siRNA in HOSE cells. siRNA oligonucleotides targeting GATA6 were transfected into HOSE or HIO cells. (A) Three days following siRNA suppression of GATA6, HIO-80 cells were analyzed by Western blotting for GATA6, Dab2, emerin, lamin A/C, and lamin B. (B) GATA6 (green) and emerin (red) were analyzed by immunofluorescence microscopy. DAPI (blue) was used to stain the nuclei. (C) Immunofluorescence analysis of lamin A/C (red) in control and GATA6 siRNA-suppressed cells. DAPI (blue) staining was used to visualize the nuclei. The area indicated by the arrow is shown at a higher magnification.

We conclude that the loss of emerin correlates well with the loss of GATA6 in ovarian cancer, and the results support the idea that loss of GATA6 results in loss of the nuclear envelope protein emerin.

**Suppression of GATA6 leads to reduction of the nuclear envelope protein emerin.** Next, we examined if suppression of GATA6 in HOSE or HIO cells might lead to the downregulation of emerin (Fig. 5). Indeed, suppression of GATA6 by the shRNA approach resulted in the reduction of Dab2, emerin, and, to a lesser degree, lamin B and lamin A/C (Fig. 5A). The loss of emerin as a consequence of GATA6 suppression was also observed by immunofluorescence microscopy in double staining experiments in which cells with large and morphologically atypical nuclei also lacked GATA6 and emerin expression (Fig. 5B). Although nuclear deformation indicated by DAPI staining was obvious, a continuous envelope covering the nuclear DNA was present, as shown by positive staining for lamin A/C (Fig. 5C).

Initially, we reasoned that emerin, like Dab2, might be one of the potentially many GATA6 transcription targets. Thus, we determined the alteration of the mRNA levels following GATA6 suppression in HOSE and HIO cells by RT-PCR. Surprisingly, in both of the HOSE lines and the one HIO line tested, the emerin mRNA level was not reduced following GATA6 suppression, although the Dab2 mRNA level was reduced (Fig. 6A). Thus, it appears that the loss of GATA6 affects emerin at the protein level rather than at the mRNA level. Indeed, when emerin or GFP-emerin was transfected and expressed in HIO cells, the exogenous emerin or GFP-emerin protein rapidly diminished upon suppression of GATA6 by siRNA. Thus, emerin loss following GATA6 suppression is likely the consequence of an increase in emerin degradation.

We also attempted to restore emerin expression in emerin-negative ovarian cancer cells. Upon transfection, the exogenous GFP-emerin fusion protein could be expressed in NIHOVCAR3 cells, but the level of the expressed protein declined steadily with time (Fig. 6B). Drug (G418)-selected clones showed neither a GFP fluorescence signal under fluorescence microscopy nor the presence of the GFP-emerin protein by Western blotting. A similar outcome was observed in OV5 ovarian cancer cells (Fig. 6C), although in parallel controls the fluorescence signals of the transfected GFP-histone H2B persisted over the same time course. In this experiment, we also observed the fluctuation of emerin protein levels at various times and under

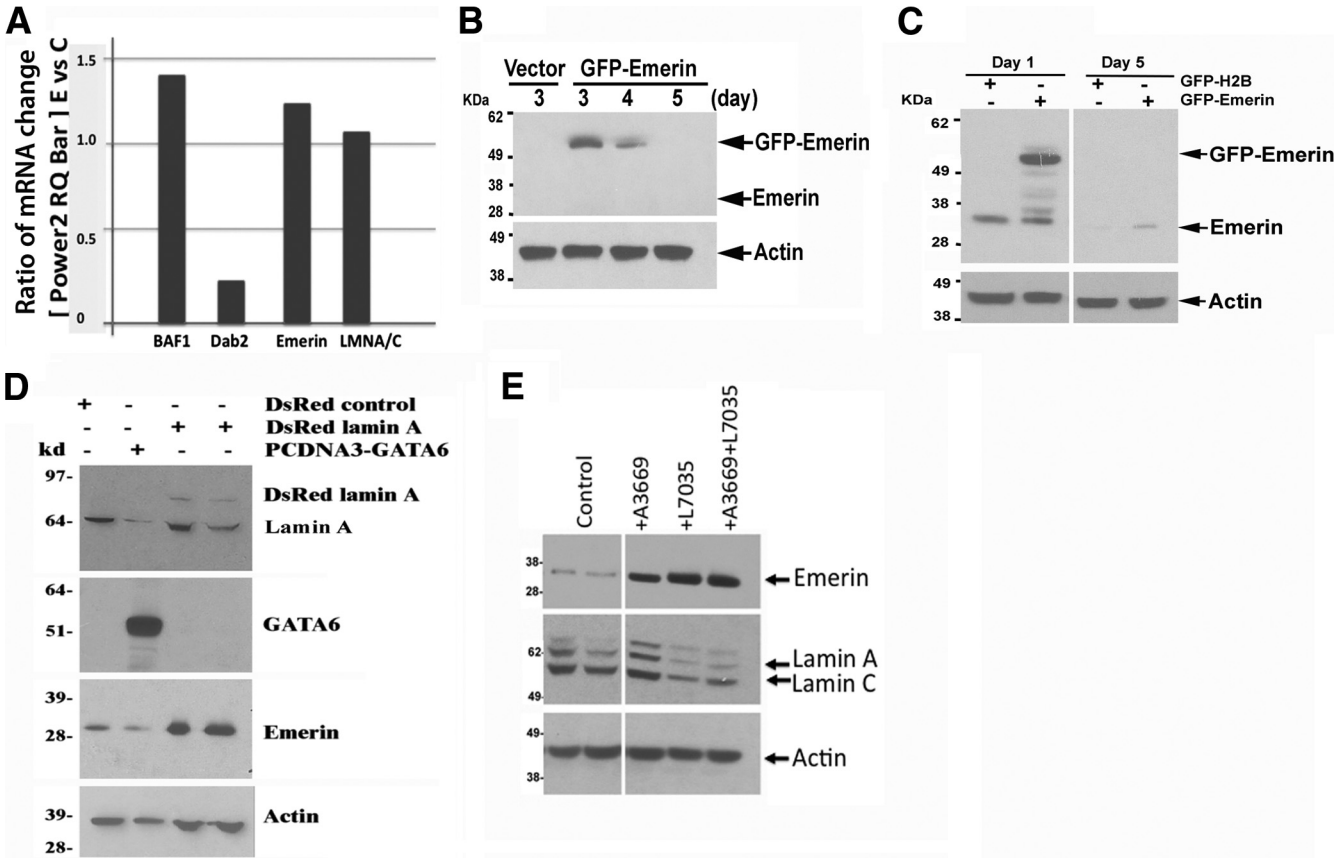


FIG. 6. Regulation of emerin mRNA and protein levels. (A) siRNA oligonucleotides targeting GATA6 were transfected into HIO cells. The mRNA levels of Baf1, Dab2, emerin, and lamin A/C were measured by real-time RT-PCR. The results are expressed as $n^2$ for the ratio of the experiment group (E, GATA6 siRNA) to the control group (C, scrambled oligonucleotide). (B) NIHOVCAR3 ovarian cancer cells were transfected with a GFP-emerin expression vector or a control vector. On days 3, 4, and 5 following transfection, a well of the transfected cells was harvested for the analysis of emerin and GFP-emerin by Western blotting. (C) OV5 ovarian cancer cells were transfected with a GFP-emerin expression vector or a GFP-histone H2B vector. On day 5 following transfection, a well of the transfected cells was harvested for the analysis of emerin and GFP-emerin by Western blotting. (D) OV5 ovarian cancer cells were transfected with a GATA6 or a Ds-Red–lamin A expression vector. On day 5 following transfection, the transfected cells were harvested for the analysis of emerin and GFP-emerin by Western blotting. Two independent Ds-Red–emerin transfection samples were analyzed. (E) OV5 ovarian cancer cells were treated with the caspase-6 inhibitor A3669 or/and the proteasome inhibitor L7035 for 48 h. The cells were then harvested for Western blot analysis of the lamin A and emerin proteins. The upper band in the lamin A/C blot (about 65 kDa) is pro-lamin A.

various culture conditions; a small amount of endogenous emerin was detected on day 1 following transfection but not on day 5 (Fig. 6C).

In experiments exploring potential factors regulating emerin expression levels, we found that transfection of GATA6 failed to restore emerin expression (Fig. 6D). Expression of lamin A (Ds-Red fusion protein) increased the emerin protein level in OV5 cells (Fig. 6D). Among several inhibitors tested, the caspase-6 inhibitor A3669 and the proteasome inhibitor L7035 increased emerin protein levels in OV5 cells (Fig. 6E). In contrast, the lamin A/C level decreased in the presence of the proteasome inhibitor (Fig. 6E).

We also determined if these protease inhibitors could block emerin loss upon GATA6 suppression in HIO and HOSE cells. Both A3669 and L7035 appeared to slow the decline of GFP-emerin upon GATA6 suppression in HIO cells, as observed by fluorescence microscopy. However, the toxicity of these compounds to HIO and HOSE cells in longer experimental time courses prevented us from analyzing the reversion of the phenotypes upon GATA6 suppression in detail.

These results suggest that both the interaction with nuclear lamina and the levels of cellular protease activities can influence emerin protein levels.

**Suppression of emerin leads to mitotic defects and formation of aneuploid cells.** The consequence of emerin depletion was then examined in HOSE and HIO cells. Western blot analysis indicated that emerin protein was suppressed by siRNA oligonucleotides (Fig. 7A). Most of the cells took up siRNA oligonucleotides, as indicated by cy3-siRNA labeling, and a significant number of cells possessing aberrant nuclear morphology were evident (Fig. 7B). GATA6 and Dab2 were still detectable in these emerin-suppressed cells (Fig. 7C). As a specificity control, downregulation of another nuclear envelope structural protein, lamin B, did not lead to atypical nuclear morphology (Fig. 7D), consistent with the lack of a role for lamin B in maintaining the nuclear shape (26). In three

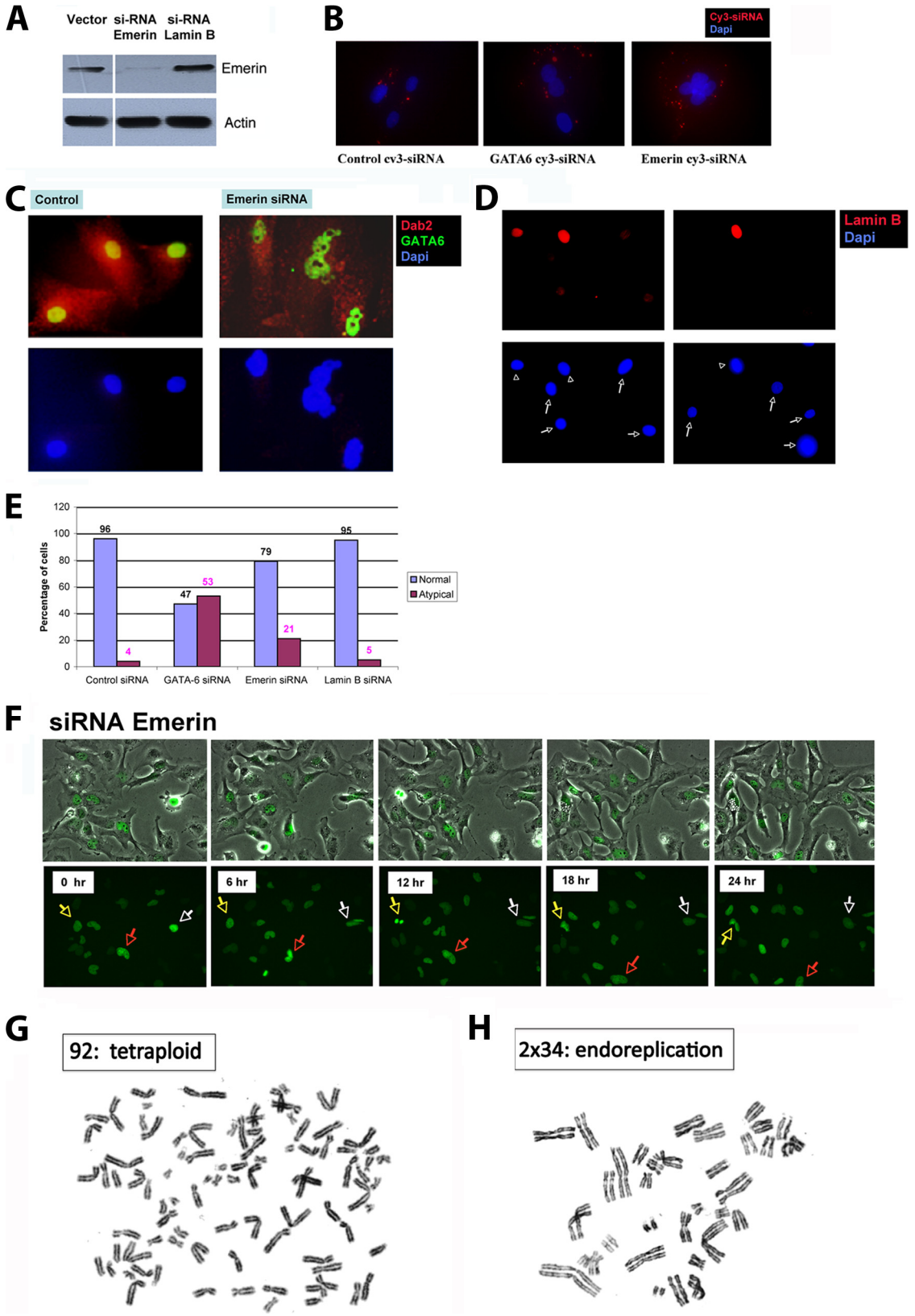


FIG. 7. Suppression of emerin expression leads to atypical nuclear morphology and polyploidy in HOSE cells. (A) Western blotting was used to determine emerin protein levels following the addition of siRNA oligonucleotides targeting emerin or a scrambled control to HOSE cells for 3 days. Actin was used as a protein loading control. (B) The presence of cy3-siRNA around the nuclei (DAPI, blue) indicates the uptake of siRNA oligonucleotides. (C) Immunofluorescence staining of control and emerin siRNA-suppressed HOSE cells with GATA6 (green), Dab2 (red), and

independent experiments in which random fields of about 100 cells were counted, approximately 20% of the emerin-suppressed cells had abnormal nuclei, compared to 4% of the cells treated with scrambled oligonucleotide controls. In comparison, GATA6 downregulation appeared to cause a more dramatic increase in cells with atypical nuclear morphology (Fig. 7E).

A defect in cytokinesis similar to that produced by GATA6 suppression was observed in emerin-suppressed HOSE or HIO cells examined by time-lapse video microscopy (Fig. 7F). The mitotic phenotype monitored by histone H2B-GFP showed that the dividing nuclei of emerin-suppressed cells regressed to form presumably 4n nuclei (Fig. 7F, arrows). We estimate that about one-third of the emerin-suppressed cells exhibited abnormal mitosis and failed cytokinesis. We examined the ploidy of the emerin-suppressed cells by a cytogenetic approach. Among 50 metaphase chromosome spreads counted, 6 tetraploid or nearly tetraploid spreads were found (Fig. 7G). Interestingly, an additional four metaphase spreads showed a signature of endoreplication in which the DNA was duplicated within each pair of parallel but separate chromosomes (Fig. 7H). In parallel experiments, GATA6 suppression resulted in 11 tetraploid or nearly tetraploid metaphase spreads, and 2 potential aneuploid (chromosomes 45 and 91) metaphase spreads were found in controls transfected with scrambled siRNA. Similar results were obtained with an additional independent HOSE cell preparation. It appears that emerin suppression also resulted in tetraploidy and also a high rate of endoreplication, which was also observed occasionally in GATA6-suppressed cells and in OV5 cells. Based on a relatively small number of cytogenetic analyses, we are not yet be able to conclude that endoreplication is a specific feature of emerin suppression or also a common consequence of GATA6 suppression. Nevertheless, we are able to conclude that the loss of emerin accounts for, at least in part, the mechanism of the nuclear deformation and formation of tetraploidy and aneuploidy as a consequence of GATA6 loss.

## DISCUSSION

Previously, we found that GATA6 expression is lost in ovarian cancer and that the subsequent loss of Dab2, a GATA6 transcription target, may be the cause of the morphological transformation of ovarian surface epithelial cells in tumorigenesis (8, 10). GATA6 was also identified by the gene trapping of mouse glioma model as the product of an astrocytoma tumor suppressor gene (3, 22). GATA6 likely has many additional transcriptional targets, and the loss of expression of these genes may also contribute to phenotypes caused by the loss of GATA6 in tumorigenesis.

In the present investigation of the phenotype of loss of GATA6 in cultured cells, we found two dramatic consequences of GATA6 suppression in ovarian surface epithelial cells: deformed nuclear morphology and the formation of aneuploid cells. The loss of emerin following GATA6 suppression was determined to account for the molecular basis of these two phenotypes. Although suppression of emerin in ovarian surface epithelial cells leads to nuclear morphological deformation and aneuploidy, the severity is not as drastic as that seen when GATA6 is suppressed. Thus, loss of emerin may account for only part of the phenotypes caused by the loss of GATA6.

**Molecular basis of nuclear deformation of cancer cells.** Enlarged and deformed nuclei are characteristics of cancer cells, and the aberrant nuclear morphology correlates with malignancy and is a diagnostic indicator (12, 56). The enlarged size of the nucleus is apparently caused by an increase in DNA content as a result of aneuploidy of cancer cells. However, the molecular cause of nuclear morphological deformation, deviating from the smooth and oval shape found in normal cells, was not previously known.

The alteration of nuclear matrix proteins has been speculated to be the underlying mechanism of the morphological deformation of malignant cells (38, 56). Since a strong correlation between nuclear morphological deformation and malignancy exists, the functional significance of nuclear morphology in cancer development and progression was also speculated about (1, 38, 56).

Loss of nuclear envelope structure proteins such as lamin A/C (26) or emerin (27, 44) causes nuclear morphological deformation, but a link to the malignant nuclear morphology of cancer cells has not been made previously. Our present finding of the loss of emerin protein provides an explanation for the nuclear deformation of ovarian cancer cells.

**Link between nuclear deformation and chromosome instability.** The present finding establishes a link between nuclear morphological deformation and aneuploidy (as a result of chromosomal instability), two consistent features of cancer cells. Presumably, a defective and weakened nuclear envelope may facilitate the loss of chromosomes through the budding and breaking off of nuclear envelope materials and the formation of micronuclei. Such a phenomenon was observed in the time-lapse video of GATA6-suppressed cells. A more prominent mechanism is the frequent mitotic failure of GATA6- and/or emerin-depleted cells. Mitotic failure leads to the

DAPI (blue) was performed. (D) Immunofluorescence staining of lamin B (red) and DAPI (blue) was performed in lamin B siRNA-suppressed HOSE cells. Two images are shown. Nuclei corresponding to lamin B-positive and -negative cells are indicated by arrowheads and arrows, respectively. (E) Summary of the comparison of nuclear morphology in HOSE cells treated with siRNA targeting a nonspecific control, GATA6, emerin, and lamin B. About 100 DAPI-stained cells from each treatment were analyzed. (F) Time-lapse images of HIO-80 cells transfected with histone H2B-GFP-expressing constructs and siRNA oligonucleotides targeting emerin. Time-lapse video microscopy was used to monitor the mitotic phenotype of GFP-expressing cells 24 h following transfection. GFP fluorescence and corresponding phase-contrast images of time courses obtained from the time-lapse video are shown. Mitotic failure and formation of abnormal nuclei were observed in multiple cells, as shown by three examples (indicated by red, yellow, and white arrows, respectively). (G) Metaphase spreads of emerin-suppressed HOSE cells. HOSE cells were transfected with control or emerin siRNA and subjected to cytogenetic analysis on day 3. Fifty consecutive chromosome spreads of each sample were selected for chromosome counting. Two representative metaphase spreads are shown: G, tetraploid (92 pairs of chromosomes); H, endoreplication ($2 \times 34$ pairs of chromosomes). Similar results were observed in an additional independent HOSE cell preparation.

formation of tetraploid cells, and aneuploidy develops in subsequent divisions of the tetraploid cells. In human cells, the role of nuclear envelope proteins in mitosis has only been revealed recently by the study of mutations in progeria syndrome (6, 11), though the mechanism of action of the nuclear envelope protein in cytokinesis and mitosis has not been well understood.

**Conserved roles of nuclear envelope proteins in nuclear morphology and mitosis.** The biological roles of nuclear envelope proteins have been best studied in *Caenorhabditis elegans* (17). Mutation or loss of function in several nuclear envelope structure proteins, including emerin and Man1 (29), Baf (31, 54), and lamin (30), in *C. elegans* produces similar nuclear and mitotic phenotypes, such as an enlarged and deformed nucleus, deficient chromosome segregation, and the formation of chromatin bridges between divided nuclei, suggesting a critical role for the nuclear envelope in cytokinesis and mitosis. In *Xenopus* egg extracts, Baf was shown to play a critical role in nuclear envelope formation (47). In mammalian cells, loss or mutation of emerin (27, 44) or lamin A/C (26) produces nuclear morphological deformation. The roles of these nuclear envelope proteins in cytokinesis and mitosis have also started to be revealed; Baf is required for chromatin condensation and segregation (31, 46), and mutations in lamin A/C interfere with mitosis and cell cycle progression (6, 11). Loss of emerin appears to influence centrosome localization (45), and a defect in cytokinesis was observed in the present study in emerin-suppressed cells. These findings are consistent with roles for these nuclear envelope proteins in both maintaining the nuclear structure and mediating cytokinesis/mitosis across species.

**Roles of emerin in cellular functions and diseases.** The role of emerin defects in muscular dystrophy has been well characterized (2, 37, 52), and the roles for emerin in cell signaling, transcriptional regulation, and regulation of retroviral infectivity have also been described (18, 20, 33). The present data add yet another corollary to emerin deficiency, i.e., genomic instability in cancer.

Emerin-deficient mice have only minimal developmental abnormalities (39); nevertheless, embryonic fibroblasts from emerin-deficient mice exhibit an abnormal nuclear shape and impaired mechanotransduction (27, 44). Possibly, the phenotype for the absence of emerin in whole animals may not be obvious due to compensation by additional nuclear envelope proteins. In our experiments, we were able to obtain polyploid/aneuploid ovarian surface epithelial cells following GATA6 or emerin suppression and maintain them in long-term culture. When we implanted these cells into immunocompromised mice, we were not able to demonstrate tumor development from them (data not shown). Thus, it is possible that chromosomal instability resulting from GATA6 or emerin suppression is not sufficient for tumorigenesis.

**Significance of these findings and unanswered questions.** In summary, the present study of the phenotype due to suppression of GATA6 in ovarian cancer cells leads to the finding of the molecular defect in the nuclear envelope of ovarian cancer cells. In the present study, the phenotypes due to GATA6 deficiency were well studied in cultured HOSE cells. The next important experiment needs to verify if these phenotypes are also present in vivo. GATA6 knockout mice die at an early embryonic stage because of failed primitive endoderm formation (5). Thus, a conditional knockout mouse model of GATA6 in ovarian surface epithelial cells is needed to perform this experiment.

We found a correlation between the absence of GATA6 and the absence of emerin in ovarian surface epithelial and cancer cells in tumor tissues. Especially, siRNA suppression of GATA6 leads to a loss of emerin in ovarian surface epithelial cells. However, we also found that the correlation between the levels of GATA6 and emerin expression is not universal; there are both cell lines and tumors that are positive for GATA6 but not for emerin or are negative for GATA6 but positive for emerin. Additionally, we found that suppression of GATA6 leads to a loss of emerin protein but not mRNA, indicating that GATA6 does not regulate emerin transcription. The preliminary results suggest that both the emerin-interacting protein lamin A/C and the cellular protease activities can influence emerin protein levels. GATA6 suppression may alter nuclear envelope structure, leading to changes in the environment of the emerin protein and its subsequent degradation. Alternatively, GATA6 suppression may increase nuclear protease activity or accessibility to emerin. Thus, the relationship between GATA6 and emerin is likely indirect and complex and is still not clear.

Nevertheless, the present finding that emerin is lost in a large percentage of ovarian cancer cell lines and tumors by itself is interesting and potentially significant. This is the first report of the finding of a molecular defect, loss of emerin, that may explain the nuclear deformation and aneuploidy of ovarian cancer cells. Nuclear envelope defects are known to cause misshapen nuclei (27, 44) and genomic instability (7), which are conspicuous in cancer cells. The present finding that a structural defect in the nuclear envelope leads to aberrant nuclear morphology and the formation of tetraploidy/aneuploidy represents a novel mechanism for the development of chromosomal instability in carcinogenesis.

## ACKNOWLEDGMENTS

We acknowledge the excellent technical assistance of Jennifer Smedberg, Malgorzata Rula, Cory Staub, Carolyn Slater, and Lisa Vanderveer and secretarial assistance of Patricia Bateman. We thank Zemin Liu for metaphase preparations, Filipe Muhale for providing suggestions and advice on flow cytometric analysis, Sandra Jablonski for help with immunofluorescence and time-lapse video microscopy, and James Oesterlitz for flow cytometric analysis. We thank our colleagues Elizabeth Smith, Robert Moore, and Corrado Caslini for reading, suggestions, and comments during the course of our experiments and the preparation of the manuscript.

These studies were supported by funds from grants R01 CA095071 and CA79716 to X. X. Xu from NCI, NIH. This work was also supported by the Fox Chase Cancer Center (Ovarian Cancer SPORE P50 CA83638; principal investigator, R. F. Ozols).

## REFERENCES

1. **Bignold, L. P.** 2003. Pathogenetic mechanisms of nuclear pleomorphism of tumour cells based on the mutator phenotype theory of carcinogenesis. Histol. Histopathol. **18:**657–664.
2. **Bione, S., E. Maestrini, S. Rivella, M. Mancini, S. Regis, G. Romeo, and D. Toniolo.** 1994. Identification of a novel X-linked gene responsible for Emery-Dreifuss muscular dystrophy. Nat. Genet. **8:**323–327.
3. **Bleau, A. M., and E. C. Holland.** 2007. Trapping the mouse genome to hunt human alterations. Proc. Natl. Acad. Sci. USA **104:**7737–7738.
4. **Boveri, T.** 1914. Zur Frage der Enstehung maligner Tumoren. Gustav Fischer Verlag, Jena, Germany.
5. **Cai, K. Q., C. D. Capo-chichi, M. E. Rula, D.-H. Yang, and X. X. Xu.** 2008. Dynamic GATA6 expression in primitive endoderm formation and maturation in early mouse embryogenesis. Dev. Dyn. **237:**2820–2829.

6. **Cao, K., B. C. Capell, M. R. Erdos, K. Djabali, and F. S. Collins.** 2007. A lamin A protein isoform overexpressed in Hutchinson-Gilford progeria syndrome interferes with mitosis in progeria and normal cells. Proc. Natl. Acad. Sci. USA **104:**4949–4954.
7. **Capell, B. C., and F. S. Collins.** 2006. Human laminopathies: nuclei gone genetically awry. Nat. Rev. Genet. **7:**940–952.
8. **Capo-chichi, C. D., I. H. Roland, L. Vanderveer, R. Bao, T. Yamagata, H. Hirai, C. Cohen, T. C. Hamilton, A. K. Godwin, and X. X. Xu.** 2003. Anomalous expression of epithelial differentiation-determining GATA factors in ovarian tumorigenesis. Cancer Res. **63:**4967–4977.
9. **Capo-chichi, C. D., M. E. Rula, J. L. Smedberg, L. Vanderveer, M. S. Parmacek, E. E. Morrisey, A. K. Godwin, and X. X. Xu.** 2005. Perception of differentiation cues by GATA factors in primitive endoderm lineage determination of mouse embryonic stem cells. Dev. Biol. **286:**574–586.
10. **Caslini, C., C. D. Capo-chichi, I. H. Roland, E. Nicolas, A. T. Yeung, and X. X. Xu.** 2006. Histone modifications silence the GATA transcription factor genes in ovarian cancer. Oncogene **25:**5446–5461.
11. **Dechat, T., T. Shimi, S. A. Adam, A. E. Rusinol, D. A. Andres, H. P. Spielmann, M. S. Sinensky, and R. D. Goldman.** 2007. Alterations in mitosis and cell cycle progression caused by a mutant lamin A known to accelerate human aging. Proc. Natl. Acad. Sci. USA **104:**4955–4960.
12. **Deligdisch, L., A. J. Einstein, D. Guera, and J. Gil.** 1995. Ovarian dysplasia in epithelial inclusion cysts. A morphometric approach using neural networks. Cancer **76:**1027–1034.
13. **Duesberg, P.** 2005. Does aneuploidy or mutation start cancer? Science **307:**41.
14. **Fearon, E. R., and B. Vogelstein.** 1990. A genetic model for colorectal tumorigenesis. Cell **61:**759–767.
15. **Fujiwara, T., M. Bandi, M. Nitta, E. V. Ivanova, R. T. Bronson, and D. Pellman.** 2005. Cytokinesis failure generating tetraploids promotes tumorigenesis in p53-null cells. Nature **437:**1043–1047.
16. **Ganem, N. J., Z. Storchova, and D. Pellman.** 2007. Tetraploidy, aneuploidy and cancer. Curr. Opin. Genet. Dev. **17:**157–162.
17. **Gorjánácz, M., A. Jaedicke, and I. W. Mattaj.** 2007. What can Caenorhabditis elegans tell us about the nuclear envelope? FEBS Lett. **581:**2794–2801.
18. **Gruenbaum, Y., A. Margalit, R. D. Goldman, D. K. Shumaker, and K. L. Wilson.** 2005. The nuclear lamina comes of age. Nat. Rev. Mol. Cell Biol. **6:**21–31.
19. **Hanahan, D., and R. A. Weinberg.** 2000. The hallmarks of cancer. Cell **100:**57–70.
20. **Jacque, J. M., and M. Stevenson.** 2006. The inner-nuclear-envelope protein emerin regulates HIV-1 infectivity. Nature **441:**641–645.
21. **Jefford, C. E., and I. Irminger-Finger.** 2006. Mechanisms of chromosome instability in cancers. Crit. Rev. Oncol. Hematol. **59:**1–14.
22. **Kamnasaran, D., B. Qian, C. Hawkins, W. L. Stanford, and A. Guha.** 2007. *GATA6* is an astrocytoma tumor suppressor gene identified by gene trapping of mouse glioma model. Proc. Natl. Acad. Sci. USA **104:**8053–8058.
23. **Kanda, T., K. F. Sullivan, and G. M. Wahl.** 1998. Histone-GFP fusion protein enables sensitive analysis of chromosome dynamics in living mammalian cells. Curr. Biol. **8:**377–385.
24. **Knudson, A. G.** 2001. Two genetic hits (more or less) to cancer. Nat. Rev. Cancer **1:**157–162.
25. **Koutsourakis, M., A. Langeveld, R. Patient, R. Beddington, and F. Grosveld.** 1999. The transcription factor GATA6 is essential for early extraembryonic development. Development **126:**723–732.
26. **Lammerding, J., L. G. Fong, J. Y. Ji, K. Reue, C. L. Stewart, S. G. Young, and R. T. Lee.** 2006. Lamins A and C but not lamin B1 regulate nuclear mechanics. J. Biol. Chem. **281:**25768–25780.
27. **Lammerding, J., J. Hsiao, P. C. Schulze, S. Kozlov, C. L. Stewart, and R. T. Lee.** 2005. Abnormal nuclear shape and impaired mechanotransduction in emerin-deficient cells. J. Cell Biol. **170:**781–791.
28. **Lengauer, C., K. W. Kinzler, and B. Vogelstein.** 1998. Genetic instabilities in human cancers. Nature **396:**643–649.
29. **Liu, J., K. K. Lee, M. Segura-Totten, E. Neufeld, K. L. Wilson, and Y. Gruenbaum.** 2003. MAN1 and emerin have overlapping function(s) essential for chromosome segregation and cell division in Caenorhabditis elegans. Proc. Natl. Acad. Sci. USA **100:**4598–4603.
30. **Liu, J., T. Rolef Ben-Shahar, D. Riemer, M. Treinin, P. Spann, K. Weber, A. Fire, and Y. Gruenbaum.** 2000. Essential roles for Caenorhabditis elegans lamin gene in nuclear organization, cell cycle progression, and spatial organization of nuclear pore complexes. Mol. Biol. Cell **11:**3937–3947.
31. **Margalit, A., M. Segura-Totten, Y. Gruenbaum, and K. L. Wilson.** 2005. Barrier-to-autointegration factor is required to segregate and enclose chromosomes within the nuclear envelope and assemble the nuclear lamina. Proc. Natl. Acad. Sci. USA **102:**3290–3295.
32. **Margolis, R. L.** 2005. Tetraploidy and tumor development. Cancer Cell **8:**353–354.
33. **Markiewicz, E., K. Tilgner, N. Barker, M. van de Wetering, H. Clevers, M. Dorobek, I. Hausmanowa-Petrusewicz, F. C. Ramaekers, J. L. Broers, W. M. Blankesteijn, G. Salpingidou, R. G. Wilson, J. A. Ellis, and C. J. Hutchison.** 2006. The inner nuclear membrane protein emerin regulates beta-catenin activity by restricting its accumulation in the nucleus. EMBO J. **25:**3275–3285.
34. **Michor, F., Y. Iwasa, B. Vogelstein, C. Lengauer, and M. A. Nowak.** 2005. Can chromosomal instability initiate tumorigenesis? Semin. Cancer Biol. **15:**43–49.
35. **Molkentin, J. D.** 2000. The zinc finger-containing transcription factors GATA-4, -5, and -6. Ubiquitously expressed regulators of tissue-specific gene expression. J. Biol. Chem. **275:**38949–38952.
36. **Morrisey, E. E., Z. Tang, K. Sigrist, M. M. Lu, F. Jiang, H. S. Ip, and M. S. Parmacek.** 1998. GATA6 regulates HNF4 and is required for differentiation of visceral endoderm in the mouse embryo. Genes Dev. **12:**3579–3590.
37. **Nagano, A., R. Koga, M. Ogawa, Y. Kurano, J. Kawada, R. Okada, Y. K. Hayashi, T. Tsukahara, and K. Arahata.** 1996. Emerin deficiency at the nuclear membrane in patients with Emery-Dreifuss muscular dystrophy. Nat. Genet. **12:**254–259.
38. **Nickerson, J. A.** 1998. Nuclear dreams: the malignant alteration of nuclear architecture. J. Cell. Biochem. **70:**172–180.
39. **Ozawa, R., Y. K. Hayashi, M. Ogawa, R. Kurokawa, H. Matsumoto, S. Noguchi, I. Nonaka, and I. Nishino.** 2006. Emerin-lacking mice show minimal motor and cardiac dysfunctions with nuclear-associated vacuoles. Am. J. Pathol. **168:**907–917.
40. **Pihan, G., and S. J. Doxsey.** 2003. Mutations and aneuploidy: co-conspirators in cancer? Cancer Cell **4:**89–94.
41. **Rajagopalan, H., M. A. Nowak, B. Vogelstein, and C. Lengauer.** 2003. The significance of unstable chromosomes in colorectal cancer. Nat. Rev. Cancer **3:**695–701.
42. **Rajagopalan, H., and C. Lengauer.** 2004. Aneuploidy and cancer. Nature **432:**338–341.
43. **Rous, P.** 1967. The challenge to man of the neoplastic cell. Science **157:**24–28.
44. **Rowat, A. C., J. Lammerding, and J. H. Ipsen.** 2006. Mechanical properties of the cell nucleus and the effect of emerin deficiency. Biophys. J. **91:**4649–4664.
45. **Salpingidou, G., A. Smertenko, I. Hausmanowa-Petrucewicz, P. J. Hussey, and C. J. Hutchison.** 2007. A novel role for the nuclear membrane protein emerin in association of the centrosome to the outer nuclear membrane. J. Cell Biol. **178:**897–904.
46. **Segura-Totten, M., A. K. Kowalski, R. Craigie, and K. L. Wilson.** 2002. Barrier-to-autointegration factor: major roles in chromatin decondensation and nuclear assembly. J. Cell Biol. **158:**475–485.
47. **Segura-Totten, M., and K. L. Wilson.** 2004. BAF: roles in chromatin, nuclear structure and retrovirus integration. Trends Cell Biol. **14:**261–266.
48. **Shi, Q., and R. W. King.** 2005. Chromosome nondisjunction yields tetraploid rather than aneuploid cells in human cell lines. Nature **437:**1038–1042.
49. **Storchova, Z., and D. Pellman.** 2004. From polyploidy to aneuploidy, genome instability and cancer. Nat. Rev. Mol. Cell Biol. **5:**45–54.
50. **Vogelstein, B., E. R. Fearon, S. R. Hamilton, S. E. Kern, A. C. Preisinger, M. Leppert, Y. Nakamura, R. White, A. M. Smits, and J. L. Bos.** 1988. Genetic alterations during colorectal-tumor development. N. Engl. J. Med. **319:**525–532.
51. **Weaver, B. A., and D. W. Cleveland.** 2006. Does aneuploidy cause cancer? Curr. Opin. Cell Biol. **18:**658–667.
52. **Wilson, K. L.** 2000. The nuclear envelope, muscular dystrophy and gene expression. Trends Cell Biol. **10:**125–129.
53. **Yang, D. H., E. R. Smith, C. Cohen, H. Wu, C. Patriotis, A. K. Godwin, T. C. Hamilton, and X. X. Xu.** 2002. Molecular events associated with dysplastic morphologic transformation and initiation of ovarian tumorigenicity. Cancer **94:**2380–2392.
54. **Zheng, R., R. Ghirlando, M. S. Lee, K. Mizuuchi, M. Krause, and R. Craigie.** 2000. Barrier-to-autointegration factor (BAF) bridges DNA in a discrete, higher-order nucleoprotein complex. Proc. Natl. Acad. Sci. USA **97:**8997–9002.
55. **Zimonjic, D. B., M. W. Brooks, N. Popescu, R. A. Weinberg, and W. C. Hahn.** 2001. Derivation of human tumor cells in vitro without widespread genomic instability. Cancer Res. **61:**8838–8844.
56. **Zink, D., A. H. Fischer, and J. A. Nickerson.** 2004. Nuclear structure in cancer cells. Nat. Rev. Cancer **4:**677–687.